

# *Ab initio* calculation of the Hoyle state

Evgeny Epelbaum<sup>a</sup>, Hermann Krebs<sup>a</sup>, Dean Lee<sup>b</sup>, Ulf-G. Meißner<sup>c,d</sup>

<sup>a</sup>*Institut für Theoretische Physik II, Ruhr-Universität Bochum, D-44870 Bochum, Germany*

<sup>b</sup>*Department of Physics, North Carolina State University, Raleigh, NC 27695, USA*

<sup>c</sup>*Helmholtz-Institut für Strahlen- und Kernphysik and Bethe Center  
for Theoretical Physics, Universität Bonn, D-53115 Bonn, Germany*

<sup>d</sup>*Institut für Kernphysik, Institute for Advanced Simulation and Jülich Center for Hadron Physics,  
Forschungszentrum Jülich, D-52425 Jülich, Germany*

The Hoyle state plays a crucial role in the hydrogen burning of stars heavier than our sun and in the production of carbon and other elements necessary for life. This excited state of the carbon-12 nucleus was postulated by Hoyle [1] as a necessary ingredient for the fusion of three alpha particles to produce carbon at stellar temperatures. Although the Hoyle state was seen experimentally more than a half century ago [2, 3] nuclear theorists have not yet uncovered the nature of this state from first principles. In this letter we report the first *ab initio* calculation of the low-lying states of carbon-12 using supercomputer lattice simulations and a theoretical framework known as effective field theory. In addition to the ground state and excited spin-2 state, we find a resonance at  $-85(3)$  MeV with all of the properties of the Hoyle state and in agreement with the experimentally observed energy. These lattice simulations provide insight into the structure of this unique state and new clues as to the amount of fine-tuning needed in nature for the production of carbon in stars.

PACS numbers: 21.10.Dr, 21.30.-x, 21.45-v, 21.60.De, 26.20.Fj

In stars with central temperatures above  $15 \times 10^6$  K, the carbon-nitrogen-oxygen cycle is the dominant process for the conversion of hydrogen into helium [4, 5]. However a key catalyst in this cycle is the carbon-12 nucleus which itself must be produced by fusion of three helium-4 nuclei or alpha particles. Without additional help this triple alpha reaction is highly suppressed at stellar temperatures and presents a bottleneck shutting down other process. Fortunately several coincidences prevent this from happening. The first stage fusing together two alpha particles is enhanced by the beryllium-8 ground state, a resonance very near the double alpha threshold. In order to enhance the fusion of the third alpha particle, Hoyle postulated a new excited state of  $^{12}\text{C}$ , a spinless even-parity resonance very near the  $^8\text{Be}$ -alpha threshold [1]. Soon after this prediction, the state was found at Caltech [2, 3] and has been investigated in laboratories worldwide. Given its role in the formation of life-essential elements, this state is commonly mentioned in anthropic arguments explaining the fine-tuning of fundamental parameters of the universe [6].

The Hoyle state presents a major challenge for nuclear theory. There have been recent studies of carbon-12 and the Hoyle state built from clusters of alpha particles [7–9]. While these empirical models provide qualitative insights, investigations of the fundamental properties of the Hoyle state require calculations from first principles. One very interesting calculation is based on fermionic molecular dynamics, but it requires a fit to properties of a broad range of nuclei to pin down the various model parameters [9]. In recent years several *ab initio* approaches have been used to calculate the binding, structure, and reactions of atomic nuclei. These in-

clude the no-core shell model [10, 11], constrained-path Green’s function Monte Carlo [12, 13], auxiliary-field diffusion Monte Carlo [14], and coupled cluster methods [15]. Despite spectacular progress over the past few years, there have been no calculations so far which reproduce the Hoyle state from first principles.

In this letter we report new *ab initio* calculations of the low-lying spectrum of carbon-12 using the framework of chiral effective field theory and Monte Carlo lattice simulations. Effective field theory (EFT) is an organizational tool which reconstructs the interactions of particles as a systematic expansion in powers of particle momenta. Initiated by Weinberg in 1991 [16], chiral EFT provides a systematic hierarchy of the forces among protons and neutrons. This approach comes with an estimate of the theoretical uncertainty at any given order which can be systematically reduced at higher orders. Over the past two decades, chiral EFT has proven a reliable and precise tool to describe the physics of few-nucleon systems. A recent review can be found in Ref. [17]. The low-energy expansion of EFT is organized in powers of  $Q$ , where  $Q$  denotes the typical momentum of particles. The momentum scale  $Q$  is also roughly the same size as the mass of the pion times the speed of light. The most important contributions come at leading order (LO) or  $O(Q^0)$ . The next most important terms are at next-to-leading order (NLO) or  $O(Q^2)$ . The terms just beyond this are next-to-next-to-leading order (NNLO) or  $O(Q^3)$ . In the lattice calculations presented here, we consider all possible interactions up to  $O(Q^3)$ . We also separate out explicitly the  $O(Q^2)$  terms which arise from electromagnetic interactions (EM) and isospin symmetry breaking (IB) due to mass differences of the up and down quarks.

Lattice effective field theory combines EFT with numerical lattice methods in order to investigate larger systems. Space is discretized as a periodic cubic lattice with spacing  $a$  and length  $L$ , where  $L$  is typically  $\sim 10$  fm. In the time direction, the time step is denoted  $a_t$  with total propagation time  $L_t$ . On this spacetime lattice, nucleons are point-like particles on lattice sites. Interactions due to the exchange of pions and multi-nucleon operators are generated using auxiliary fields. Lattice EFT was originally used to calculate the properties of homogeneous nuclear and neutron matter [18, 19]. Since then the ground state energies of atomic nuclei with up to twelve nucleons have been investigated [20, 21]. A recent review of the literature can be found in Ref. [22].

In the lattice calculations presented here we use the low-energy filtering properties of Euclidean time propagation. If  $H$  is the Hamiltonian operator for a quantum system, then the eigenvalues of  $H$  are the energy levels and the eigenvectors of  $H$  are the corresponding wavefunctions. For any given quantum state,  $\Psi$ , the projection amplitude  $Z_\Psi(t)$  is defined as the expectation value  $\langle e^{-Ht} \rangle_\Psi$ . For large Euclidean time  $t$ , the exponential operator  $e^{-Ht}$  enhances the signal of low-energy states. The corresponding energies can be determined from the exponential decay of these projection amplitudes.

In Table I we present lattice results for the ground state energies of  ${}^4\text{He}$ ,  ${}^8\text{Be}$ , and  ${}^{12}\text{C}$ . The method of calculation is essentially the same as that described in Ref. [21]. We note that higher-order corrections are computed using perturbation theory. Some improvements have been made which eliminate the problem of overbinding found in Ref. [21]. One significant improvement involves choosing local two-derivative lattice operators at NLO which prevent interactions tuned at low momenta from becoming too strong at the cutoff momentum. Further details will be discussed in a forthcoming publication. We show results at leading order (LO), next-to-leading order (NLO), next-to-leading order with isospin-breaking and electromagnetic corrections (IB + EM), and next-to-next-to-leading order (NNLO). We follow the power counting scheme used in Ref. [21], and there is no additional isospin-breaking and electromagnetic corrections at NNLO. All energies are in units of MeV. For comparison we also give the experimentally observed energies. These calculations as well as all other results presented here use lattice spacing  $a = 1.97$  fm and time step  $a_t = 1.32$  fm. To simplify unit conversions we are using units where  $\hbar$  and  $c$ , the speed of light, are set equal to 1. The error bars in Table I are one standard deviation estimates which include both Monte Carlo statistical errors and uncertainties due to extrapolation at large Euclidean time. For each simulation we have collected data from 2048 processors each generating about 300 independent lattice configurations. In the case of  ${}^{12}\text{C}$ , these configurations are stored on disk and used for the analysis of excited states described later.

TABLE I: Lattice results for the ground state energies for  ${}^4\text{He}$ ,  ${}^8\text{Be}$ , and  ${}^{12}\text{C}$ . For comparison we also exhibit the experimentally observed energies. All energies are in units of MeV.

	${}^4\text{He}$	${}^8\text{Be}$	${}^{12}\text{C}$
LO [ $O(Q^0)$ ]	-24.8(2)	-60.9(7)	-110(2)
NLO [ $O(Q^2)$ ]	-24.7(2)	-60(2)	-93(3)
IB + EM [ $O(Q^2)$ ]	-23.8(2)	-55(2)	-85(3)
NNLO [ $O(Q^3)$ ]	-28.4(3)	-58(2)	-91(3)
Experiment	-28.30	-56.50	-92.16

For  ${}^4\text{He}$  the periodic cube length is  $L = 9.9$  fm, while the system size for the  ${}^8\text{Be}$  and  ${}^{12}\text{C}$  calculations are each 11.8 fm. By probing the two-nucleon spatial correlations for each nucleus, we conclude that the finite size corrections are smaller than the combined statistical and extrapolation error bars. Since the lattice EFT calculations are based upon an expansion in powers of momentum, the size of corrections from  $O(Q^0)$  to  $O(Q^2)$  and from  $O(Q^2)$  to  $O(Q^3)$  give an estimate of systematic errors due to omitted terms at  $O(Q^4)$  and higher. We have used the experimentally observed  ${}^4\text{He}$  energy to set one of the unknown three-nucleon interaction coefficients at NNLO commonly known in the literature as  $c_D$ . However, the results for  ${}^8\text{Be}$  and  ${}^{12}\text{C}$  are predictions without free parameters, and the results at NNLO are in agreement with experimental values.

In order to compute the low-lying excited states of carbon-12, we generalize the Euclidean time projection method to a multi-channel calculation. We apply the exponential operator  $e^{-Ht}$  to 24 single-nucleon standing waves in the periodic cube. From these standing waves we build initial states consisting of 6 protons and 6 neutrons each and extract four orthogonal energy levels with the desired quantum properties. All four have even parity and total momentum equal to zero. Three states have  $z$ -axis component of angular momentum,  $J_z$ , equal to 0, and one has  $J_z$  equal to 2. We note that the lattice discretization of space and periodic boundaries reduce the full rotational group to a cubic subgroup. As a consequence only 90-degree rotations along axes are exact symmetries. This complicates the identification of spin states. However the degeneracy or non-degeneracy of energy levels for  $J_z = 0$  and  $J_z = 2$  allows one to distinguish between spinless states and spin-2 states. We use the spectroscopic notation  $J_n^\pi$ , where  $J$  is the total spin,  $\pi$  denotes parity, and  $n$  labels the excitation starting from 1 for the lowest level. In this notation the ground state is  $0_1^+$ , the Hoyle state is  $0_2^+$ , and the lowest spin-2 state is  $2_1^+$ .

In Table II we show results for the low-lying excited states of  ${}^{12}\text{C}$  at leading order (LO), next-to-leading order (NLO), next-to-leading order with isospin-breaking and electromagnetic corrections (IB + EM), and next-to-

TABLE II: Lattice results for the low-lying excited states of  $^{12}\text{C}$ . For comparison the experimentally observed energies are shown. All energies are in units of MeV.

	$0_2^+$	$2_1^+, J_z = 0$	$2_1^+, J_z = 2$
LO [ $O(Q^0)$ ]	-94(2)	-92(2)	-89(2)
NLO [ $O(Q^2)$ ]	-82(3)	-87(3)	-85(3)
IB + EM [ $O(Q^2)$ ]	-74(3)	-80(3)	-78(3)
NNLO [ $O(Q^3)$ ]	-85(3)	-88(3)	-90(4)
Experiment	-84.51	-87.72	

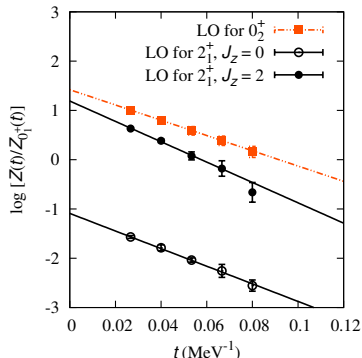


FIG. 1: Extraction of the excited states of  $^{12}\text{C}$  from the time dependence of the projection amplitude at LO. The slope of the logarithm of  $Z(t)/Z_{0_1^+}(t)$  at large  $t$  determines the energy relative to the ground state.

next-to-leading order (NNLO). All energies are in units of MeV. For comparison we list the experimentally observed energies. As before the error bars in Table II are one standard deviation estimates which include both Monte Carlo statistical errors and uncertainties due to extrapolation at large Euclidean time. Systematic errors due to omitted higher-order interactions can be estimated from the size of corrections from  $O(Q^0)$  to  $O(Q^2)$  and from  $O(Q^2)$  to  $O(Q^3)$ . In Fig. 1 we show lattice results used to extract the excited state energies at leading order. For each excited state we plot the logarithm of the ratio of the projection amplitudes,  $Z(t)/Z_{0_1^+}(t)$ , at leading order.  $Z_{0_1^+}(t)$  is the ground state projection amplitude, and the slope of the logarithmic function at large  $t$  gives the energy difference between the ground state and the excited state.

As seen in Table II and summarized in Fig. 2, the NNLO results for the Hoyle state and spin-2 state are in agreement with the experimental values. While the ground state and spin-2 state have been calculated in other studies [10, 11, 13], these results are the first *ab initio* calculations of the Hoyle state with an energy close to the phenomenologically important  $^8\text{Be}$ -alpha threshold. Experimentally the  $^8\text{Be}$ -alpha threshold is at  $-84.80$  MeV, and the lattice determination at NNLO

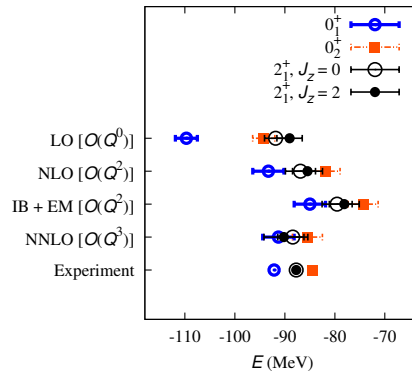


FIG. 2: Summary of lattice results for the carbon-12 spectrum and comparison with the experimental values. For each order in chiral EFT labelled on the left, results are shown for the ground state (blue circles), Hoyle state (red squares), and the  $J_z = 0$  (open black circles) and  $J_z = 2$  (filled black circles) projections of the spin-2 state.

gives  $-86(2)$  MeV. We also note the energy level crossing involving the Hoyle state and the spin-2 state. The Hoyle state is lower in energy at LO but higher at NLO. One of the main characteristics of the NLO interactions is to increase the repulsion between nucleons at short distances. This has the effect of decreasing the binding strength of the spinless states relative to higher-spin states. We note the 17 MeV reduction in the ground state binding energy and 12 MeV reduction for the Hoyle state while less than half as much binding correction for the spin-2 state. This degree of freedom in the energy spectrum suggests that at least some fine-tuning of parameters is needed to set the Hoyle state energy near the  $^8\text{Be}$ -alpha threshold. It would be very interesting to understand which fundamental parameters in nature control this fine-tuning. At the most fundamental level there are only a few such parameters, one of the most interesting being the masses of the up and down quarks [23, 24].

Our comments on the binding energies at LO would also suggest that the nuclear wavefunctions at LO are probably somewhat too compact for the spinless states. We check for this explicitly by computing the proton-proton radial distribution function  $f_{pp}(r)$ . Using any given proton as a reference point, the function  $f_{pp}(r)$  is proportional to the probability of finding a second proton at a distance  $r$ . For macroscopic liquids the radial distribution function is normalized to 1 at asymptotically large distances. In our finite system we instead normalize the integral of  $f_{pp}(r)$  over all space to equal  $1 - Z^{-1}$ , where  $Z$  is the total number of protons. In Fig. 3 we show the radial distribution function  $f_{pp}(r)$  at Euclidean time  $t = 0.08$  MeV $^{-1}$  for the ground state (A), Hoyle state (B), and the  $J_z = 0$  (C) and  $J_z = 2$  (D) projections of the spin-2 state. The yellow bands denote one standard

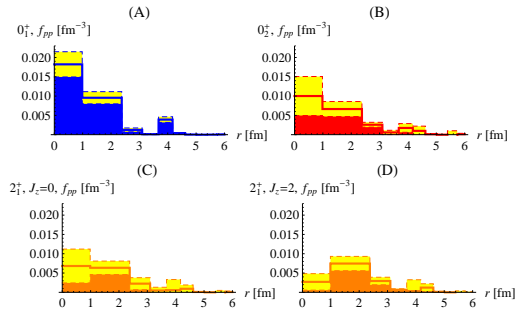


FIG. 3: The radial distribution function  $f_{pp}(r)$  for the ground state (A), Hoyle state (B), and in the  $J_z = 0$  (C) and  $J_z = 2$  (D) projections of the spin-2 state. The yellow bands denote error bars.

deviation error bars.

The ground state is very compact with a large central core. The Hoyle state and spin-2 state look qualitatively similar, though the Hoyle state has a slightly larger central core. A secondary maximum near  $r \simeq 4$  fm is visible in the ground state and each of the excited states. This secondary maximum seems to arise from configurations where three alpha clusters are arranged approximately linearly. More calculations are planned to confirm whether this configuration is physically important or just a lattice artifact.

It is straightforward to compute the root-mean-square charge radius from the second moment of  $f_{pp}(r)$ . We include the charge radius of the proton, 0.84 fm [25], by adding it in quadrature. At LO we obtain a charge radius of 2.04(2) fm for the ground state, 2.4(1) fm for the Hoyle state, and 2.6(1) fm and 2.4(2) fm for  $J_z = 0$  and  $J_z = 2$  projections of the spin-2 state. The experimentally observed charge radius for the ground state is 2.47(2) fm [26]. As expected the ground state wavefunction at LO is too small by a proportion similar to the overbinding in energy. The radius for the ground state and Hoyle state should increase significantly when the NLO corrections are included. One expects some correction due to the finite-volume periodic boundary. At LO the tail of the radial distribution function suggests that this is a rather small effect for  $L = 11.8$  fm. Higher order corrections to the radial distribution function, charge radii, as well as electromagnetic transition strengths are currently under investigation and will be discussed in a future publication.

In summary we have presented *ab initio* calculations of the low-lying states of carbon-12 using lattice effective field theory. In addition to the ground state and excited spin-2 state, we find a resonance with spin zero and positive parity at  $-85(3)$  MeV which appears to be the Hoyle state. Much more work is needed and planned,

including calculations at smaller lattice spacings. But these lattice calculations provide a new opening towards understanding the physics of this unique state and may also prove useful for the study of other nuclear reactions relevant to the element synthesis in stars.

**Acknowledgements** We thank Steven Weinberg for useful communications. Financial support acknowledged from the DFG (SFB/TR 16), Helmholtz Association (VH-VI-231), BMBF (grant 06BN9006), U.S. DOE (DE-FG02-03ER41260), EU HadronPhysics2 project “Study of strongly interacting matter”, and ERC project 259218 NUCLEAREFT. Computational resources provided by the Jülich Supercomputing Centre at the Forschungszentrum Jülich.

- 
- [1] F. Hoyle, *Astrophys. J. Suppl. Ser.* **1**, 121 (1954).
  - [2] D. N. F. Dunbar, R. E. Pixley, W. A. Wenzel and W. Whaling, *Phys. Rev.* **92**, 649 (1953).
  - [3] C. W. Cook, *et al.*, *Phys. Rev.* **107**, 508 (1957).
  - [4] C. F. von Weizsäcker, *Phys. Z.* **39**, 633 (1938).
  - [5] H. A. Bethe, *Phys. Rev.* **55** 434 (1939).
  - [6] H. Kragh, *Arch. Hist. Exact Sci.* **64**, 721 (2010).
  - [7] P. Descouvemont, *J. Phys. G: Nucl. Part. Phys.* **35** 014006 (2008).
  - [8] A. Tohsaki, H. Horiuchi, P. Schuck and G. Röpke, *Phys. Rev. Lett.* **87**, 192501 (2001); T. Yamada, *et al.*, arXiv:1103.3940 [nucl-th].
  - [9] M. Chernykh, *et al.*, *Phys. Rev. Lett.* **98**, 032501 (2007).
  - [10] P. Navratil, J. P. Vary and B. R. Barrett, *Phys. Rev. Lett.* **84**, 5728 (2000).
  - [11] P. Maris, J. P. Vary and A. M. Shirokov, *Phys. Rev. C* **79**, 014308 (2009).
  - [12] S. C. Pieper, and R. B. Wiringa, *Ann. Rev. Nucl. Part. Sci.* **51**, 53 (2001)
  - [13] S. C. Pieper, *Bull. Am. Phys. Soc.* **54**, 70 (2009).
  - [14] S. Gandolfi, F. Pederiva, and S. Fantoni, and K. E. Schmidt, *Phys. Rev. Lett.* **99**, 022507 (2007).
  - [15] G. Hagen, T. Papenbrock, D. J. Dean, and M. Hjorth-Jensen, *Phys. Rev. Lett.* **101**, 092502 (2008).
  - [16] S. Weinberg, *Nucl. Phys. B* **363**, 3 (1991).
  - [17] E. Epelbaum, H. W. Hammer and U.-G. Meißner, *Rev. Mod. Phys.* **81**, 1773 (2009).
  - [18] H. M. Muller, S. E. Koonin, R. Seki and U. van Kolck, *Phys. Rev. C* **61**, 044320 (2000).
  - [19] D. Lee, B. Borasoy and T. Schäfer, *Phys. Rev. C* **70**, 014007 (2004).
  - [20] E. Epelbaum, H. Krebs, D. Lee and U.-G. Meißner, *Eur. Phys. J. A* **40**, 199 (2009).
  - [21] E. Epelbaum, H. Krebs, D. Lee and U.-G. Meißner, *Phys. Rev. Lett.* **104**, 142501 (2010); *Eur. Phys. J. A* **45**, 335 (2010).
  - [22] D. Lee, *Prog. Part. Nucl. Phys.* **63**, 117 (2009).
  - [23] S. R. Beane and M. J. Savage, *Nucl. Phys. A* **713**, 148 (2003).
  - [24] E. Epelbaum, U.-G. Meißner and W. Glöckle, *Nucl. Phys. A* **714**, 535 (2003).
  - [25] R. Pohl, *et al.*, *Nature* **466**, 213 (2010).
  - [26] F. Ajzenberg-Selove, *Nucl. Phys. A* **506**, 1 (1990).